Accepted Manuscript

Synthesis, characterization of bay-substituted perylene diimide based D-A-D type small molecules and its applications as a non-fullerene electron acceptor in polymer solar cells

Ramasamy Ganesamoorthy, Rajagopalan Vijayaraghavan, K. Ramki, Pachagounder Sakthivel

PII: S2468-2179(17)30164-8

DOI: 10.1016/j.jsamd.2017.11.005

Reference: JSAMD 134

To appear in: *Journal of Science: Advanced Materials and Devices*

Received Date: 1 September 2017

Revised Date: 15 November 2017

Accepted Date: 19 November 2017

Please cite this article as: R. Ganesamoorthy, R. Vijayaraghavan, K. Ramki, P. Sakthivel, Synthesis, characterization of bay-substituted perylene diimide based D-A-D type small molecules and its applications as a non-fullerene electron acceptor in polymer solar cells, *Journal of Science: Advanced Materials and Devices* (2017), doi: 10.1016/j.jsamd.2017.11.005.

Synthesis, characterization of bay-substituted perylene diimide based D-A-D type small molecules and its applications as a non-fullerene electron acceptor in polymer solar cells

Ramasamy Ganesamoorthy[1], Rajagopalan Vijayaraghavan[1], K. Ramki[2], and Pachagounder Sakthivel[2]*

[1]*Department of Chemistry, School of Advanced Sciences, VIT University, Vellore-632 014, Tamil Nadu, India.*

[2*]*Department of Nanoscience and Technology, Bharathiar University, Coimbatore- 641 046, Tamilnadu, India.*

[*]Corresponding author: Tel: (+91-9677560890) E-mail: polysathi@gmail.com

Synthesis, characterization of bay-substituted perylene diimide based D-A-D type small molecules and its applications as a non-fullerene electron acceptor in polymer solar cells

Abstract

We report a series of bay substituted perylene diimide based donor-acceptor-donor (D-A-D) type small molecule acceptor derivatives such as S-I, S-II, S-III and S-IV, for the small molecule based organic solar cell (SM-OSC) applications. The electron rich thiophene derivatives such as, thiophene, 2-hexylthiophene, 2,2'-bithiophene, and 5-hexyl-2,2'-bithiophene, were used as donor (D) and perylene diimide was used as an acceptor (A). The synthesized small molecules were confirmed by FT-IR, NMR, and HR-MS. The small molecules showed wide and strong absorption in the UV-vis region up to 750 nm, it reduced the optical band gap to < 2 eV. The calculated highest occupied molecular orbital (HOMO), lowest unoccupied molecular orbital (LUMO) were comparable with the $PC_{61}BM$. Scanning electron microscope (SEM) studies confirmed the aggregation in the small molecules S-I to S-IV. Small molecules showed thermal stability up to 300 °C. In bulk heterojunction organic solar cell (BHJ-OSCs), S-I based device showed a maximum power conversion efficiency (PCE) of 0.12% with P3HT polymer donor. The PCE was declined with respect to the number of thiophene units and the flexible alkyl chain in the bay position.

Keywords: Perylene diimide; Donor-Acceptor; Small molecule; Non-fullerene; Suzuki coupling.

1. Introduction

Perylene diimide (PDI) based conjugated small molecules and polymers have received considerable attention in the academic research and industrial application such as, organic field effect transistors (OFETs), fluorescent solar collectors, electro-photographic devices, laser dyes, and OSCs, due to their cost-effective, stability, easy molecular engineering process for excellent physical, optical, and electronic properties [**1-2**]. In the OSCs field, fullerene derivatives are most widely used as an acceptors. Though modified fullerene acceptor based OSCs showed excellent results, price,

solubility, low absorption properties, necessitated the need for non-fullerene acceptors[**3**]. Various non-fullerene acceptors such as rylene diimide (RDI), naphthalene diimide (NDI), and perylene diimide (PDI) based copolymers or small molecule [**4**] acceptors, diketopyrrolopyrrole and benzothiadiazole based acceptors [**5-6**]. Even though a sizeable non-fullerene acceptors are used, PDIs are the most widely studied non-fullerene acceptors in the OSCs.

In the recent past extensive research and review articles are reported on the PDIs in OSCs and OFET field. In 2011, Zhou et al., conveyed D-A type polymers which containing the vinylene, thiophene, dithieno[3,2b:2',3'-d]pyrrole, fluorene, dibenzosilole, and carbazole units as donors and perylene diimide unit as acceptors and achieved PCE range between 0.11-0.29% [**7**] in all polymer solar cells with P3HT polymer donor but the device fabricated with PT-1 polymer donor by using the mixture of solvents showed a maximum PCE of 2.23%. Similarly, in 2013, Zhou et al., isolated regio-regular and regio-irregular D-A type copolymers of PDI and bithiophene, the device based on the copolymers achieved a PCE of 0.45 and 0.95% respectively in conventional device structure, on the other hand the PCE was boosted to 1.55 and 2.17% [**8**] respectively in inverted device structure. Zhan et al reported a 1.08% PCE for the fused dithienothiophene and PDI based D-A type polymer with PTTV-PT polymer in all polymer solar cells [**9**]. In 2015, Dai et al reported thienylenevinylene donor and PDI acceptor based D-A type co-polymer and achieved a PCE of 1.0% with PBDTTT-CT polymer donor [**10**]. The main setback to PDI polymers is very low PCE with minimum reproducibility.

To rectify the setbacks of PDI polymer acceptors various small molecule based acceptors are reported. The significant type of PDI small molecules as follows, N-substituted symmetrical/asymmetrical PDI's, bay substituted mono or diimides, and ortho-substituted PDIs [**11**]. Out of the above PDI based small molecules, N-substituted PDIs showed a lower PCE in the range from 0.01 to 0.18% with P3HT polymer donor [**12**]. Even though ortho-substituted PDIs showed a maximum PCE of 3.62% [**13**] with PBDTT-FTTE polymer the production difficulty leads to new type of PDIs. Bay substituted PDIs based small molecules play a vital role in the non-fullerene acceptors. In the PDI based small molecule D-A-D or A-D-A type small molecules showed better results due to

the effective intramolecular charge transfer (ICT). ICT enhanced the absorption near to infrared region. Some of the bay substituted symmetrical PDIs showed a maximum PCE of 3.17% with P3HT polymer donor [**14**]. The highest PCE is comparable with the P3HT and $PC_{61}BM$ based device under similar condition. The introduction of electron rich group in the PDI core directly influenced the HOMO and LUMO energy levels of the PDI core. Hence, the easy way to tune the photo-physical property was introduction of electron rich group in the bay position. Similarly, ortho or bay bridged PDIs showed the PCE between 0.90-2.35% with P3HT polymer donor [**15**], but with other polymer donors such as PPDT2FBT it showed a maximum PCE of 5.28%. Hence, it was clear PDI based small molecule acceptors showed better PCE, reproducibility than the PDI based polymer acceptors.

Fascinated by the foresaid result, in this paper we report the synthesis, characterization and photophysical studies of bay substituted D-A-D type PDI small molecules. We studied the effect of bay substitution in UV-vis absorption, electrochemical properties, HOMO, LUMO energy level, thermal stability and surface morphology.

2. Experimental Section

2.1 Instruments and measurements.

Fourier transform-infrared (FT-IR) spectra were recorded by the KBr disc method using Shimadzu IR Affinity-1S spectrophotometer. FT-IR spectra were recorded in the transmittance mode over the range of 500-4000 cm^{-1}. UV–vis spectra were recorded with the Hitachi U-2910 spectrophotometer. UV–vis experiments were carried out for the spin cast thin film (2400 rpm) with the same instrument. Fluorescence spectra were measured by using Hitachi F-7000 fluorescence spectrophotometer. ^{1}H and ^{13}C NMR spectra were recorded on Bruker 400 MHz spectrometer using $CDCl_3$ as the solvent. The electrochemical behaviour of the small molecules were studied by using CH Instrument. Cyclic voltammogram was recorded in three electrode workstation, which containing the Platinum wire as working electrode, a standard calomel electrode, and Pt disc as counter electrode. 0.1 M tetrabutylammonium hexafluorophosphate (Bu_4NPF_6) in dichloromethane (DCM) as the supporting electrolyte at a scan rate of 50 mV s^{-1}. Thermogravimetric analysis (TGA) was conducted under the inert nitrogen atmosphere with a SDT Q600 instrument. The sample was heated at a heating

rate of 20 °C min^{-1} in the temperature range from 35 to 800 °C. HR-MS spectroscopy was recorded by using Jeol GCMS GC-Mate.

2.2 Fabrication of BHJ-OSCs

The BHJ-OSCs were fabricated using the following configuration: ITO/PEDOT:PSS/P3HT:S-I to S-IV /LiF/Al. The ITO-coated glass substrates were ultrasonically cleaned with detergent, purified deionized water, acetone, and isopropyl alcohol. The 40 nm thick PEDOT:PSS (Clevios PH1000) layer was spin-coated onto the pre-cleaned and UV- ozone treated ITO substrate followed by annealing in air at 150 °C for 30 min. The P3HT: S-I to S-IV blend was prepared in chloroform (CF), at a 1:1, weight ratio with a total blend concentration of 15 mg mL^{-1}. The blended solution was filtered with a 0.45 mm PTFE (hydrophobic) syringe filter and the active layer was spin-coated over the PEDOT:PSS modified ITO anode and dried at room temperature for 1 h. Lithium fluoride (LiF) (0.5 nm) and aluminum (Al) cathodes (100 nm) were deposited on top of the active layer under vacuum less than 5.0×10^{-6} torr to yield an active area of 9 mm^2 per pixel. The evaporation thickness was controlled by a quartz crystal sensor. The film thickness was measured with a α-Step IQ surface profiler (KLA Tencor, San Jose, CA). The performance of the BHJ-OSCs were measured using calibrated airmass (AM) 1.5G solar simulator (Oriel Sol3A Class AAA solar simulator, models 94043A) with a light intensity of 100 mW cm^{-2} adjusted using a standard PV reference cell (2 cm × 2 cm monocrystalline silicon solar cell, calibrated at NREL, Colorado, USA) and a computer controlled Keithley 236 source measure unit [**16**]. All device fabrication procedures and measurements were carried out in air at room temperature.

2.3 Materials.

High purity analytical grade (A.R) chemicals were purchased and used as received from the reputed chemical suppliers. 1, 7-dibromo-perylene-3,4,9,10-tetracarboxylic dianhydride (Br-PTCDA), N,N'bis-(2,6-diisopropylphenyl)-1,7-dibromoperylene-3,4:9,10-tetracarboxylic acid diimide (Br-PDI-IA), thiophene boronic acid pinocol esters (T-I to T-IV) were prepared from the previous reported work [**17-19**].

2.4 General procedure for the synthesis of 1,7-disubstituted PDI small molecules S-I to S-IV.

Synthesis of small molecules was shown in Fig. **1**. In a 3 neck round bottom (R. B) flask 0.433 g of Br-PDI-IA (0.5 mmol) was dissolved in 30 mL of dry THF and purged with N_2 for half an hour. To this 2 mole % $Pd(PPh_3)_4$ (0) catalyst was added. The temperature was raised to 50 °C and 5 mL of 2 M aqu. K_2CO_3 was added. Finally, to the above reaction mixture diverse thiophene boronic acid pinacol ester derivatives (T-I to T-IV), 1 mmol was added and refluxed overnight under inert N_2 atm. After, cooled to room temperature, 5 mL of 2 N HCl was added and the mixture was extracted with CH_2Cl_2, dried over Na_2SO_4, and concentrated. The residue was purified by column chromatography using 20% DCM as eluent and finally, the titled products S-I to S-IV were obtained. Appearance, percentage of yield, molecular formula (M.F.), NMR and HR-MS data for the individual compounds were given below.

2.4.1 Analytical data for the small molecule S-I.

Violet colour powder, yield-57% M.F-$C_{56}H_{46}N_2O_4S_2$. ^{1}H NMR [400 MHz, $CDCl_3$, δ=7.26 ppm, s], 8.76 (s, perylene H, 1H), 8.34-8.32 (d, perylene H, 1H), 8.21-8.19 (d, perylene H, 1H), 7.53-7.52 (d, thiophene H, 1H), 7.51-7.47 (t, thiophene H, 1H), 7.40 (broad s, thiophene H, 1H), 7.35-7.33 (d, benzene 2H, 1H), 7.22-7.21 (m, benzene 1H, 1H), 2.78-2.71 (sep, methylene H, 2H), 1.18-1.16 (d, methyl H, 12H), ^{13}C NMR [100 MHz, $CDCl_3$, δ=77.16, 3 peaks], 163.39, 163.34, (C=O), 145.67, 143.57, 136.27, 135.18, 133.85, 133.58, 130.48, 130.34, 129.86, 129.72, 129.57, 128.98, 128.70, 128.49, 127.69, 124.13, 122.44, 122.19, (aromatic carbon), 29.22, 24.07, 24.00, (isopropyl carbon). HR-MS calculated mass 874.29 and found mass 874.10.

2.4.2 Analytical data for the small molecule S-II.

Green colour solid, yield-53%, M.F-$C_{68}H_{70}N_2O_4S_2$. ^{1}H NMR [400 MHz, $CDCl_3$, δ=7.26 ppm, s], 8.65 (s, perylene H, 1H), 8.25-8.22 (s, perylene H, 2H), 7.41 (t, benzene H, 1H), 7.27-7.25 (d, benzene H, 2H), 7.17-7.11 (d, thiophene H, 1H), 6.99-6.90 (d, thiophene H, 1H), 2.81-2.77 (sep,

methylene H, 2H), 2.72-2.68 (m, methylene H, 2H), 1.64-1.61 (t, methylene H, 2H), 1.47-1.41 (m, methylene H, 6H), 1.18-1.10 (m, methylene H, 12H), 0.81-0.80 (t, methyl H, 3H), ^{13}C NMR [100 MHz, $CDCl_3$, δ=77.16, 3 peaks], 163.46, 163.42, (C=O), 149.83, 145.71, 140.91, 136.24, 135.41, 134.04, 130.06, 130.11, 129.66, 129.61, 127.44, 125.89, 124.09, 122.31, 122.10, (aromatic carbon), 31.55, 31.48, 30.34, 29.21, 28.66, 24.06, 23.98, 22.52, 14.03 (hexyl amine carbon). HR-MS calculated mass 1042.48 and found mass 1042.15.

2.4.3 Analytical data for the small molecule S-III.

Green colour solid, yield-57.8%, M.F.-$C_{64}H_{50}N_2O_4S_4$. ^{1}H NMR [400 MHz, $CDCl_3$, δ=7.26 ppm, s], 8.78-8.75 (d, perylene H, 1H), 8.46-8.36 (m, perylene H, 2H), 7.50-7.46 (t, benzene H, 1H), 7.34-7.05 (m, benzene and thiophene H, 6H), 2.76-2.73 (sep, methylene H, 2H), 1.25-1.17 (d, methyl H, 12H). ^{13}C NMR [100 MHz, $CDCl_3$, δ=77.16, 3 peaks], 162.28 (C=O), 144.61, 141.03, 139.64, 135.49, 135.08, 132.07, 129.46, 128.70, 127.55, 127.06, 124.36, 124.13, 123.53, 123.10, 121.45 (aromatic carbons), 28.68, 28.17, 23.06, 22.98. HR-MS calculated mass 1038.27 and found mass 1038.12.

2.4.4 Analytical data for the small molecule S-IV.

Green colour solid, yield-48%, M.F-$C_{76}H_{74}N_2O_4S_4$. ^{1}H NMR [400 MHz, $CDCl_3$, δ=7.26 ppm, s], 8.77 (s, perylene H, 1H), 8.46-8.44 (d, perylene H, 1H), 8.37-8.35 (d, perylene H, 1H), 7.35-7.33 (d, benzene H, 1H), 7.30-7.29 (d, thiophene H, 3H), 7.18-7.17 (d, thiophene H, 1H), 7.04-7.03 (d, thiophene H, 1H), 6.71-6.70 (d, thiophene H, 1H), 2.81-2.75 (m, methylene H, 4H), 1.67-1.69 (m, methylene H, 2H), 1.32-1.18 (m, methylene H, 12H), 1.17-1.16 (d, methylene H, 12H), 0.90-0.87 (t, methyl H, 3H), ^{13}C NMR [100 MHz, $CDCl_3$, δ=77.16, 3 peaks], 163.35, 163.33, (C=O), 146.70, 145.67, 141.34, 133.89, 133.54, 130.43, 129.70, 128.69, 128.54, 125.07, 124.34, 124.28, 124.12, 122.44, 122.19, (aromatic carbon), 31.57, 30.23, 29.21, 28.75, 24.00, 24.01, 22.56, 14.08 (hexyl amine carbon). HR-MS calculated mass 1206.45 and found mass 1206.24.

3. Results and Discussion

3.1 Synthesis and characterization

The synthetic pathway to the Br-PDI-IA and diverse thiophene boronic acid pinocol ester derivatives T-I to T-IV were followed from the previous reports [**17-19**]. In the first step thiophene boronic acid pinocol ester derivatives were synthesized from the diverse thiophene derivative in the presence of n-butyl lithium and 2-isopropoxy-4,4',5,5'-tetramethyl-1,3,2-dioxaborolane at -78 °C in dry THF solvent under the inert N_2 gas atmosphere. In the second step Br-PDI-IA was prepared by the N-alkylation between Br-PTCDA and 2,6-diisopropylaniline in propionic acid as described in previous literature in good yields. Finally, small molecule S-I to S-IV were synthesized by Suzuki coupling method between the diverse thiophene boronic acid pinocol ester derivatives and Br-PDI-IA. The small molecules were easily soluble in most of the organic solvents, especially in the DCM and $CHCl_3$. ^{1}H NMR and ^{13}C NMR spectra were performed in $CDCl_3$ solution at room temperature. From data obtained from the HR-MS, ^{1}H and ^{13}C NMR, the product formation was confirmed.

3.2 FT-IR analysis

Functional group of the small molecules and starting materials were confirmed by FT-IR spectra. In the FT-IR spectra of the small molecules S-I to S-IV, the aromatic C-H stretching appeared at 2958 cm^{-1}, aliphatic C-H stretching appeared in between 2962-2868 cm^{-1}, C=O in plane asymmetric stretching appeared at 1706 cm^{-1}, C=O out-of-plane symmetric stretching appeared between 1701-1705 cm^{-1}, C=C stretching frequencies appeared between 1664-1668 cm^{-1}, C-N stretching frequencies appeared between 1394-1398 cm^{-1} and the C-S bending frequencies appeared between 1016-1056 cm^{-1}. Vibrational frequency comparison for the small molecules S-I to S-IV with Br-PDI-IA showed the drastic change in the functional group stretching frequencies [**20**]. It confirmed the formation C-C coupling bond in the perylene diimide core.

3.3 ^{1}H and ^{13}C NMR analysis

^{1}H NMR and ^{13}C NMR spectra were performed in $CDCl_3$ solution at room temperature. Apparently in the ^{1}H NMR spectra of small molecules, except S-II, the complete appearance of the perylene protons as one pair of singlet and two pairs of doublet in the range of 8.0-9.0 ppm. In case of S-II, the ^{1}H NMR spectra showed two pairs of singlet which have different intensity of the peaks in the same range. The appearance of peryelene protons in the slight upper field than compared with parent perylenediimide as one singlet and two doublets confirms the electron rich thiophene group was inducted into the perylene core structure. The 2,6-diisopropylphenyl proton signals which have one pair of triplet and doublet peak bearing the same intensity observed in the range of 7.3-7.5 ppm. In the case of S-I thiophene protons were appeared as two doublets and a triplet signals bearing the same intensity observed in the range of 7.2-7.5 ppm. In the case of S-III due to the number of thiophene unit increasing the appearance of thiophene protons as two doublets and a triplet signals bearing the same intensity was observed in the range of 7.0-7.3 ppm. S-II and S-IV showed specific one pair of doublet signal in the range of 6.87 ppm and 6.72 ppm respectively, because of the presence of hexyl group in the α-position to the oligothiophenes [**21**]. Similarly aliphatic methylene protons of small molecules were appeared as a septet in little higher field between 2.71-2.64 ppm than the Br-PDI-IA (2.79-2.69 ppm).

In the ^{13}C NMR spectra of small molecules, C=O peak appeared commonly over the range of 160 ppm. Coupling carbons appeared in the range between 135.1-135.4 ppm and the aliphatic carbons are appeared in the range between 31 ppm to 14 ppm. As the number of thiophene increases, their peaks and peaks of perylene derivatives were overlapped in range over 120 ppm. Along with disappearance of 120.9 ppm peak for C-Br present in the ^{13}C NMR spectra of the starting material Br-PDI-IA, appearance of new peaks in the region of 135.1-135.4 ppm were consistent with carbon-carbon bond formation between α-position of thiophene and PDI core.

3.4 UV-vis analysis

Absorption spectra of the small molecules S-I to S-IV were measured in $CHCl_3$ (1.0×10^{-5} M) as well as thin film are given in Fig. **2a** and their data were presented in Table **1**. As compared to the, Br-PDI-IA, the small molecules S-I to S-IV, showed the UV-vis absorptions with a bathochromic

shift. The red shift was more intense with respect to the number of thiophene unit, which was attributed to the intramolecular charge transfer between the donor and acceptor. The small molecules S-I to S-IV showed three absorption bands, first band appeared between 288 to 348 nm was recognized to the π-π* transition of the PDI core and thiophene, second band appeared between 413 to 482 nm was assigned to the electronic S_0-S_2 transition which confirms the donor thiophene substituents in the bay position, and the third band appeared between 567 to 620 nm was attributed to the S_0-S_1 transition of the conjugated thiophene moiety. The most intense absorption band of S-I and S-II were appeared at 610, and 620 nm respectively. On the other hand, S-III and S-IV showed the most intense peak at 337, and 348 nm respectively was due to extended conjugation of the bithiophene moiety. Among the thiophene (S-I and S-II) and bithiophene (S-III and S-IV) based small molecules, S-III and S-IV showed more red shift, this may be due to the S_0-S_1 transition of more conjugated bithiophene moiety. The introduction of hexyl groups into the thiophene donor, such as S-II and S-IV showed red shift with compare to S-I and S-III. This argument was supported to the highly flexible and donating character of alkyl chain length. The optical band gaps of the small molecules were calculated from the following equation (**1**) by substituting the onset absorption edge of the small molecules. The optical band gaps of the small molecules S-I to S-IV in solution state could be estimated to be 1.93, 1.85, 1.74 and 1.62 eV respectively. Solid state absorption spectra of small molecules S-I to S-IV in thin film was measured by coating a fine layer of the small molecules S-I to S-IV over the glass plate (Fig. **2b**) and the corresponding data were given in Table **1**. Absorption spectra in the film state showed the similar trends and comparable to the solution spectra. In the thin film form small molecules S-I to S-IV showed two absorption bands, first absorption band appeared between 415 to 491 nm, which was attributed to the S_0-S_2 transition and the second band was appeared between 571 to 650 nm, which was attributed to the S_0-S_1 transition respectively. There was negligible difference in the S_0-S_2 transition between the solution and solid state absorption spectra, but due to close packing he S_0-S_1 transition band showed broad absorption towards the higher wavelength region [**22**]. The broadening and red-shift of the bands resulted small band gap. The optical band gaps of the small molecules S-I to S-IV in thin film could be estimated to be 1.86, 1.72, 1.64, and 1.58 eV from the absorption edges of their UV-vis spectra.

E_g^{opt} = (1240/Onset absorption edge) eV…… (**1**).

3.5 Fluorescence property analysis (FL)

The fluorescence spectra (FL) of small molecules S-I to S-IV in $CHCl_3$ were recorded upon the different excitation wavelength and the corresponding emission values were given in the Table **1**. FL spectra of the small molecules S-I and S-II comparatively showed more intense peak, than the S-III and S-IV. The FL spectra of S-III to S-IV showed extremely weak fluorescence due to the efficient intramolecular charge transfer between the PDI donor and thiophene acceptor was shown in Fig. **3a**. Bathochromic shift was observed in the FL spectra of the small molecules from S-I to S-IV which was shown in Fig. **3b**. Emission peaks for the small molecules S-I to S-IV observed at 661, 701, 722, and 756 nm respectively. Stokes shift were calculated from the difference between the absorption and emission peak of small molecules [**23**]. Stokes shift values of the small molecules S-I to S-IV were 94, 113, 112, and 136 cm^{-1} respectively. Stokes shift values were increased with respect to the number of thiophene and hexyl group. The high electron donating thiophene moiety not only increased the absorption in the UV-vis spectra, but also declined the fluorescence than compared with parent perylenediimide dyes due to the extended conjugation of the thiophene and efficient charge transfer between the donor and acceptor.

3.6 Cyclic voltammetry (CV) analysis

CV analysis for the small molecules were performed in DCM with 0.1 M Bu_4NPF_6 as a supporting electrolyte at a scan rate of 50 mV s^{-1} in an electrochemical workstation which contains Pt wire as working electrode, Pt disc as counter electrode and Ag/AgCl reference electrode was given in Fig. **4** and the corresponding data were presented in the Table **2**. The onset oxidation and reduction potential could be used to estimate the HOMO and LUMO energy level respectively [**24**]. The onset oxidation potentials of the small molecules S-I to S-IV were 1.64, 1.49, 1.47, and 1.33 eV and the corresponding HOMO energy levels were -5.77, -5.62, -5.60, and -5.46 eV, respectively by assuming that the energy of Fc/Fc^+ was -4.8 eV. Onset reduction potential of the small molecules S-I to S-IV

were -0.27, -0.26, -0.22, and -0.21 eV and the calculated LUMO energy levels were -3.86, -3.87, -3.91, and -3.92 eV respectively. The LUMO values of the small molecules were close to the universal $PC_{61}BM$ acceptor [**3**]. The electrochemical band gaps of the S-I to S-IV could be estimated to be 1.91, 1.75, 1.69, and 1.54 eV. From the above result it was clear that the small molecules showed lower band gaps and comparable LUMO level with $PC_{61}BM$ acceptors.

3.7 Thermogravimetric analysis

Thermogravimetric analysis of the small molecules, S-I to S-IV were measured in a nitrogen atmosphere at a heating rate of 20 °C min^{-1} from 30 to 800 °C was given in Fig. **5**. Thermogravimetric analysis confirmed that the small molecules S-I to S-IV exhibited good thermal stability. The 5% weight loss of the small molecules S-I to S-IV on heating were 302, 392, 310, and 430 °C respectively. So that the small molecules S-IV was stable up to 430 °C. The high thermal stability of the small molecule was due to the rigid perylene core group [**24**]. Thermal stability was amplified with respect to number of thiophene units and alkyl chain.

3.8 Morphology analysis

Morphology of the small molecules were evaluated in the thin film. Thin films of the small molecules were prepared by a drop casting method over a glass plate in $CHCl_3$ solution (0.1 mg mL^{-1}) and the morphologies of microstructures were characterized by SEM corresponding image was shown in Fig. **6**. Thin films of the small molecules S-I to S-IV showed highly ordered structures. The SEM images displayed all of the small molecules could efficiently self-assemble into one-dimensional microstructures with different morphologies. Small molecules S-I and S-II were aggregated in flower like clusters structures with an average width of 0.2 µm and lengths up to 2 µm were obtained. Closer investigation of these larger clusters indicated that they were constructed of bundles of tiny nano-sheets. But in the case of S-III, it showed a ball like structure with random shallow traps. Although small molecules S-IV self-assembled into bundle-like micro sheets, with an average size of 2-3 µm. Aggregation property of the PDI resulted improved the surface roughness. Aggregation was also one of the important parameters which would enhance the efficient charge transport property [**25**].

3.9 Energy level comparison

Energy level diagram was constructed and compared for the small molecule with the standard P3HT donor the corresponding diagram was given in Fig. **7**. It was clear that the LUMO energy levels of the S-I to S-IV (~3.9 eV) were almost closer to the standard $PC_{61}BM$ (~ 4.2 eV) acceptor. Hence the small molecules S-I to S-IV with the low electrochemical band gap and comparable LUMO would be a very good acceptor material for the OSC application [**26**].

3.10 Photovoltaic properties analysis

The current–voltage (J–V) curves of small molecules S-I to S-IV as the sensitizers in BHJ-OSCs as cast film was shown in Fig. **8**, and corresponding open-circuit voltage (V_{oc}), short-circuit current (J_{sc}), fill factor (FF), and the PCE are shown in Table **3**. The data from the photovoltaic study revealed that the V_{oc} and J_{sc} of S-I was maximum, which resulted the highest PCE of 0.12%. The J_{sc} follows the order of S-I (0.98 mA cm^{-2}) > S-III (0.73 mA cm^{-2}) > S-III (0.26 mA cm^{-2} > S-IV (0.16 mA cm^{-2}). Obviously, the J_{sc} of dyes do not exceed 1 mA cm^{-2}, which is probably due to the narrow and short absorption spectra that limited the use of long wavelengths energy. Compared with S-II and S-IV, the J_{sc} of S-I and S-III were a little larger, which may be due to the stronger aggregation of star shaped PDI small molecules, which can produce relatively more excited state electrons. Meanwhile, the J_{sc} of small molecule S-I are higher than the rest of the small molecules, this may be due to the transmission ability of electrons in the molecule is also relatively strong. The V_{oc} of the small molecules S-I to S-IV were gradually decreased along with the order of S-II (0.43 V), > S-III (0.42 V) > S-IV (0.39 V), > S-I (0.36 V), which was attributed to the fact that their HOMO–LUMO band gaps were broaden gradually, and the excitation of sensitizers is relatively difficult. Control device was fabricated under identical condition in the following order, ITO/ PEDOT:PSS / P3HT: $PC_{61}BM$/ LiF /Al and the device based on the P3HT: $PC_{61}BM$ was showed a maximum PCE of 3.70% with a V_{oc} of 0.63 V, J_{sc} of 9.55 mA cm^{-2} and a FF of 62%. Even though the performance of the PDI small molecule was very low but it was comparable to the some of the previous reports [**12**, **27-30**]. The performance enhancement was under progress.

4. Conclusions

In summary, bay substituted D-A-D type perylene based small molecule dyes, S-I to S-IV were synthesized and characterized by FT-IR, ^{1}H NMR, ^{13}C NMR, UV-vis, FL and HR-MS studies. Small molecules S-I to S-IV showed the broad absorption, which extended up to 750 nm with good molar absorption coefficient, which ultimately reduced the band gap value to < 2 eV. The high electron donating oligothiophene derivatives not only increased the absorption in the UV-vis spectra, but also declined the fluorescence than compared with parent perylenediimide dyes due to the extended conjugation of the thiophene ring. The intramolecular charge transfer between the electron donating thiophene and electron accepting perylene diimide core resulted weak fluorescence. The small molecules showed excellent thermal stability up to 300 °C. The energy levels of $PC_{61}BM$ and small molecules S-I to S-IV were showed close resembles, but the high thermal stability, good UV-vis absorption and higher molar absorption coefficient, and lower band gap with good molar absorption coefficient, was superior to $PC_{61}BM$. As a cast film, in BHJ-OSCs small molecule S-I showed a maximum PCE of 0.12% with P3HT polymer donor. Remaining small molecules showed lower PCE than the S-I. PCE was declined with respect to number of thiophene units and alkyl chain due to the larger aggregation in solid state. The performance augmentation was under progress.

Acknowledgements

This project has been supported by the Ministry of Department of Science and Technology (DST), India, under the Science and Engineering Research Board (SERB) NO. SB/FT/CS-185/2011 and Solar Energy Research Initiative (SERI) Programme (DST/TM/SERI/FR/172(G)). We thank the VIT management for the lab and instrument facility.

References

1 X. Zhan, J. Zhang, S. Tang, Y. Lin, M. Zhao, J. Yang, H. Zhang, Q. Peng, G. Yu, Z. Li, Pyrene fused perylene diimides: Synthesis, characterization and applications in organic field-effect transistors and optical limiting with high performance, Chem. Commun. 51 (2015) 7156-7159.

2 R. Ganesamoorthy, G. Sathiyan, P. Sakthivel, Review: Fullerene based acceptors for efficient bulk heterojunction organic solar cell applications, Sol. Energy Mater. Sol. Cells, 161 (2017) 102-148.

3 P. Sakthivel, T. Won, S. Kim, S. Kim, Y. Gal, E. A. Chae, W. Suk, S. Moon, J. Lee, S. Jin, Synthesis and studies of methylester substituted thieno-o-quinodimethane fullerene multi-adducts for polymer solar cells, Sol. Energy Mater. Sol. Cells, 113 (2013) 13-19.

4 G. Bottari, G.D. Torre, D.M. Guldi, T. Torres, Covalent and noncovalent phthalocyanine-carbon nanostructure systems: Synthesis, Photoinduced electron transfer, and application to molecular photovoltaics, Chem. Rev. 110 (2010) 6768-6816.

5 R.Y.C. Shin, T. Kietzke, S. Sudhakar, A. Dodabalapur, Z. Chen, A. Sellinger, N-type conjugated materials based on 2-vinyl-4,5-dicyanoimidazoles and their use in solar cells, Chem. Mater. 19 (2007) 1892-1894.

6 M.F. Falzon, A.P. Zoombelt, M.M. Wienk, R.A. Jansen, Diketopyrrolopyrrole-based acceptor polymers for photovoltaic application, J, Phys. Chem. Chem. Phys. 13 (2011) 8931-8939.

7 E. Zhou, J. Cong, Q. Wei, K. Tajima, C. Yang, K. Hashimoto, All-polymer solar cells from perylene diimide based copolymers: Material design and phase separation control, Angew. Chem. 50 (2011) 2799-2855.

8 Y. Zhou, Q. Yan, Y. Zheng, J. Wang, D. Zhao, J. Pei, New polymer acceptors for organic solar cells: The effect of regio-regularity and device configuration, J. Mater. Chem. A, 1 (2013) 6609-6613.

9 X. Zhan, Z. Tan, E. Zhou, Y. Li, R. Misra, A. Grant, B. Domercq, X. Zhang, Z. An, X. Zhang, S. Barlow, B. Kippelen, S.R. Marder, Copolymers of perylene diimide with dithienothiophene and dithienopyrrole as electron-transport materials for all-polymer solar cells and field-effect transistors, J. Mater. Chem. 19 (2009) 5794-5803.

10 S. Dai, Y. Lin, P. Cheng, Y. Wang, X. Zhao, Q. Ling, X. Zhan, Perylene diimideethienylenevinylene-based small molecule and polymer acceptors for solution-processed fullerene-free organic solar cells, Dyes Pigm. 114 (2015) 283-289.

11 P.E. Hartnett, A. Timalsina, H.S.S.R. Matte, N. Zhou, X. Guo, W. Zhao, A. Facchetti, R.P.H. Chang, M.C. Hersam, M. Wasielewski, T.J. Marks, Slip-stacked perylenediimides as an alternative strategy for high efficiency nonfullerene acceptors in organic photovoltaics, J. Am. Chem. Soc. 136 (2014) 16345-16356.

12 W.S. Shin, H. Jeong, M. Kim, S. Jin, M. Kim, J.K. Lee, J.W. Lee, Y. Gal, Effects of functional groups at perylene diimide derivatives on organic photovoltaic device application, J. Mater. Chem. 16 (2006) 384-390.

13 P.E. Hartnett, E.A. Margulies, H.S.S.R. Matte, M.C. Hersam, T.J. Marks, M.R. Wasielewski, Effects of crystalline perylenediimide acceptor morphology on optoelectronic properties and device performance, Chem. Mater. 28 (2016) 3928-3936.

14 G.D. Sharma, M.S. Roy, J.A. Mikroyannidis, K.R.J. Thomas, Synthesis and characterization of a new perylene bisimide (PBI) derivative and its application as electron acceptor for bulk heterojunction polymer solar cells, Org. Electron. 13 (2012) 3118-3129.

15 X. Zhang, Z. Lu, L. Ye, C. Zhan, J. Hou, S. Zhang, B. Jiang, Y. Zhao, J. Huang, S. Zhang, Y. Liu, Q. Shi, Y. Liu, J. Yao, A potential perylene diimide dimer-based acceptor material for highly efficient solution-processed non- fullerene organic solar cells with 4.03% efficiency, Adv. Mater. 25 (2013) 5791-5794.

16 G.E. Park, H.J. Kim, S. Choi, D.H. Lee, M.A. Uddin, H.Y. Woo, M.J. Cho, D.H. Choi, New M- and V-shaped perylene diimide small molecules for high-performance nonfullerene polymer solar cells, Chem. Commun. 52 (2016) 8873-8876.

17 C. Kohl, T. Weil, J. Qu, K. Müllen, Towards highly fluorescent and water-soluble perylene dyes, Chem. Eur. J. 10 (2004) 5297-5310.

18 Y. Dienes, S. Durben, T. Karpati, T. Neumann, U. Englert, L. Nyulaszi, T. Baumgartner, Selective tuning of the band gap of π-conjugated dithieno[3,2-b:2’,3’-d]phospholes toward different emission colors, Chem. Eur. J. 13 (2007) 7487-7500.

19 V. Sivamurugan, K. Kazlauskas, S. Jursenas, A. Gruodis, J. Simokaitiene, J.V. Grazulevicius, S. Valiyaveettil, Synthesis and photophysical properties of glass-forming bay-substituted perylenediimide derivatives, J. Phys. Chem. B 114 (2010) 1782-1789.

20 A.F. Mansour, M.G. El-Shaarawy, S.M. El-Bashir, M.K. El-Mansy, M. Hammam, Optical study of perylene dye doped poly(methylmethacrylate) as fluorescent solar collector, Poly. Int. 51 (2002) 393-397.

21 S. Sengupta, R.K. Dubey, R.W.M. Hoek, S.P.P. van-Eeden, D.D. Gunbaş, F.C. Grozema, E.J.R. Sudhölter, W.F. Jager, Synthesis of regioisomerically pure 1,7-dibromoperylene-3,4,9,10-tetracarboxylic acid derivatives, J. Org. Chem. 79 (2014) 6655-6662.

22 C.C. Chao, M.K. Leung, Y.O. Su, K.Y. Chiu, T.H. Lin, S.J. Shieh, S.C. Lin, Photophysical and electrochemical properties of 1,7-diaryl-substituted perylene diimides, J. Org. Chem. 70 (2005) 4323-4331.

23 P. Deng, L. Liu, S. Ren, H. Li, Q. Zhang, N-acylation: An effective method for reducing the LUMO energy levels of conjugated polymers containing five-membered lactam units, Chem. Commun. 48 (2012) 6960-6962.

24 Y. Liu, Y. Wang, L. Ai, Z. Liu, X. Ouyang, Z. Ge, Perylenebisimide regioisomers: Effect of substituent position on their spectroscopic, electrochemical, and photovoltaic properties, Dyes Pigm. 121 (2015) 363-371.

25 D. Kotowski, S. Luzzati, G. Scavia, M. Cavazzini, A. Bossi, M. Catellani, E. Kozma, The effect of perylene diimides chemical structure on the photovoltaic performance of P3HT/perylene diimides solar cells, Dyes Pigm. 120 (2015) 57-64.

26 P. Sakthivel, H.S. Song, N. Chakravarthi, J.W. Lee, Y. Gal, S. Hwang, S. Jin, Synthesis and characterization of new indeno[1,2-b]indoleco-benzothiadiazole-based π-conjugated ladder type polymers for bulk heterojunction polymer solar cells, Polymer 54 (2013) 4883-4893.

27 J. Yi, Y. Ma, J. Dou, Y. Lin, Y. Wang, C.Q. Ma, H. Wang, Influence of para-alkyl chain length of the bay-phenyl unit on properties and photovoltaic performance of asymmetrical perylenediimide derivatives, Dyes Pigm. 126 (2016) 86-95.

28 A. Namepetra, E. Kitching, A.F. Eftaiha, I.G. Hill, G.C. Welch, Understanding the morphology of solution processed fullerene-free small molecule bulk heterojunction blends, Phys. Chem. Chem. Phys. 18 (2016) 12476-12485.

29 T. Adhikari, Z.G. Rahami, J.M. Nunzi, O. Lebel, Synthesis, characterization and photovoltaic performance of novel glass-forming perylenediimide derivatives, Org. Electron. 34 (2016) 146-156.

30 A.D. Hendsbee, S.M. McAfee, J.P. Sun, T.M. McCormick, I.G. Hill, G.C. Welch, Phthalimide-based π-conjugated small molecules with tailored electronic energy levels for use as acceptors in organic solar cells, J. Mater. Chem. C 3 (2015) 8904-8915.

Legends for Figure

Fig. 1 Scheme for the synthesis of small molecules S-I to S-IV.

Fig. 2 (**a)** UV-vis absorption spectra of small molecules S-I to S-IV in $CHCl_3$ solution. (**b)** in thin film.

Fig. 3 (a) FL spectra of small molecules S-I to S-IV in $CHCl_3$ (1×10^{-5} M) (**b)** bathochromic shift in FL spectra

Fig. 4 (**a**) Cyclic voltammograms of small molecules S-I and S-II (**b**) S-III and S-IV in DCM solution with 0.1 M Bu_4NPF_6 as supporting electrolyte, at a scan speed of 50 mV s^{-1} (vs. Fc/Fc^+)

Fig. 5 TGA graph for the small molecules S-I to S-IV at a scan rate of 20 °C minutes

Fig. 6 SEM images of small molecules S-I to S-IV

Fig. 7 Energy level comparison diagram for small molecules S-I to S-IV

Fig. 8 Photovoltaic properties of small molecules S-I to S-IV with P3HT polymer donor in BHJ-OSCs

Table 1 UV-vis data for the small molecules S-I to S-IV in $CHCl_3$ solution (1×10^{-5} M) and film.

Small molecule	λ^{abs} in (sol) nm	$\varepsilon = \times 10^4$ L $mol^{-1}.cm^{-1}$ (sol)	λ^{abs} (film) nm	λ^{emi}_{max} (sol) nm	λ^{onset}_{abs} (sol) nm	λ^{onset}_{abs} (film) nm	E_g^{opt} (sol) eV	E_g^{opt} (film) eV

S-I	288, 413, 567	8.5, 3.4, 8	415, 572	661	641	666	1.93	1.86
S-II	289, 433, 588	17, 7.9, 12	435, 592	701	670	720	1.85	1.72
S-III	337, 466, 610	19, 10, 8.2	471, 631	722	713	754	1.74	1.64
S-IV	348, 482, 620	22, 17, 7.6	491, 650	756	765	784	1.62	1.58

Sol-Solution, Ɛ-molar absorption coefficient, λ_{abs} -absorption wavelength, $\lambda_{\max}^{emi}$ -emission maximum, λ_{abs}^{onset} -absorption onset

Table 2 Electrochemical properties comparison for the small molecules S-I to S-IV in DCM.

Small molecule	red-2	red-1	oxi-1	oxi-2	E_{onset}^{red} eV	E_{onset}^{ox} eV	HOMO (eV)[a]	LUMO (eV)[b]	E_g^{ele} (eV)[c]	E_g^{opt} (eV)[d]
S-I	-0.71	-0.33	1.76	1.88	-0.27	1.64	-5.77	-3.86	1.91	1.93
S-II	-0.84	-0.32	1.64	1.72	-0.26	1.49	-5.62	-3.87	1.75	1.85
S-III	-0.73	-0.28	1.55	1.81	-0.22	1.47	-5.60	-3.91	1.69	1.74
S-IV	-0.58	-0.27	1.40	1.82	-0.21	1.33	-5.46	-3.92	1.54	1.62

a. HOMO = – (4.8 – $E_{1/2}$, $Fc/Fc^+ + E_{onset}^{ox}$) b. LUMO = – (4.8 – $E_{1/2}$, $Fc/Fc^+ + E_{onset}^{red}$) c. Redox potential for small molecules were measured in DCM with 0.1 M Bu_4NPF_6 with a scan rate of 50 mV s^{-1} (vs. Fc/Fc^+). d. = (1240/ absorption edge) eV in solution.

Table 3 Photovoltaic performances of PDI based small molecules S-I to S-IV with P3HT polymer donor in BHJ-OSCs under the illumination of 1.5G, 100 mW cm^{-2}. (ITO/ PEDOT:PSS / P3HT: S-I to S-IV/ LiF /Al)

Small molecule	V_{oc}	J_{sc} (mA Cm^{-2})	FF (%)	PCE (%)
S-I	0.36	0.98	34	0.12
S-II	0.43	0.26	14	0.01

S-III	0.42	0.73	21	0.06
S-IV	0.39	0.16	25	0.02

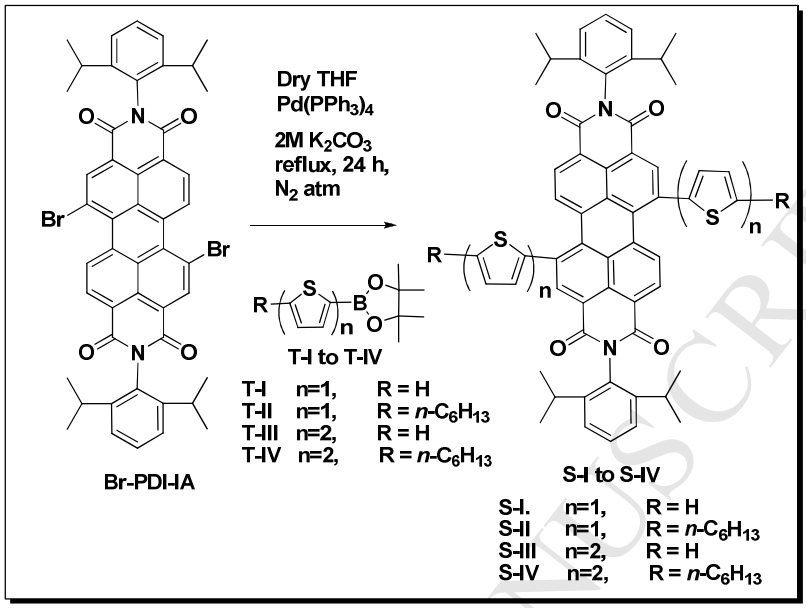
Dry THF
Pd(PPh3)4
2M K2CO3
reflux, 24 h,
N2 atm
Br-PDI-IA
T-I to T-IV
T-I n=1, R = H
T-II n=1, R = n-C6H13
T-III n=2, R = H
T-IV n=2, R = n-C6H13
S-I to S-IV
S-I. n=1, R = H
S-II n=1, R = n-C6H13
S-III n=2, R = H
S-IV n=2, R = n-C6H13

Fig. 1

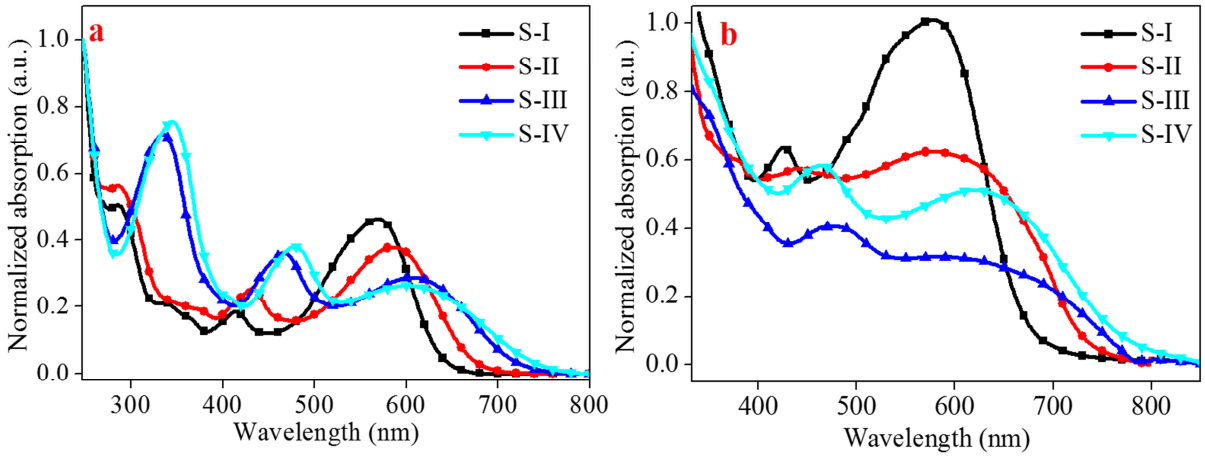
a
b
S-I
S-II
S-III
S-IV
Normalized absorption (a.u.)
Wavelength (nm)

Fig. 2

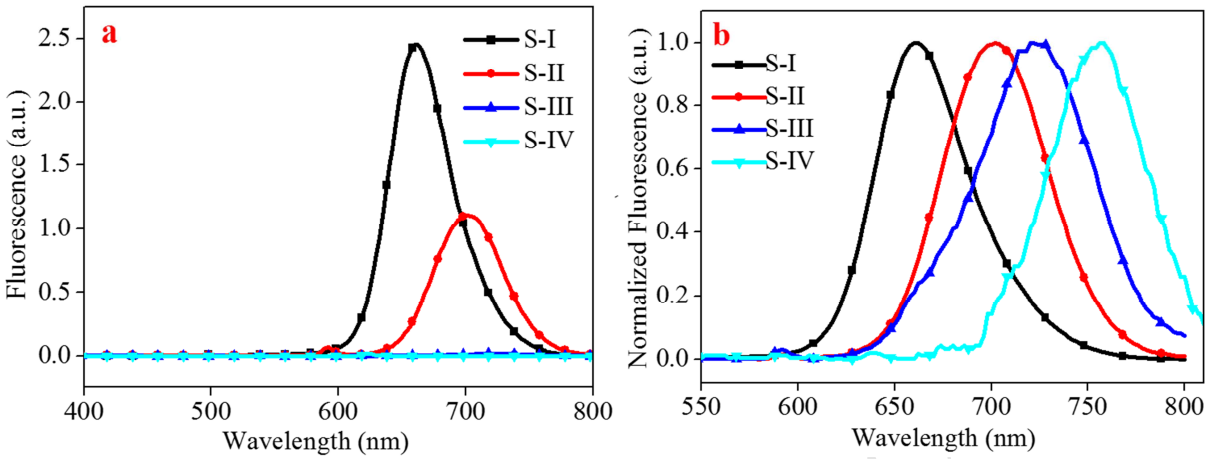
a
S-I
S-II
S-III
S-IV
Fluorescence (a.u.)
Wavelength (nm)
b
S-I
S-II
S-III
S-IV
Normalized Fluorescence (a.u.)
Wavelength (nm)

Fig. 3

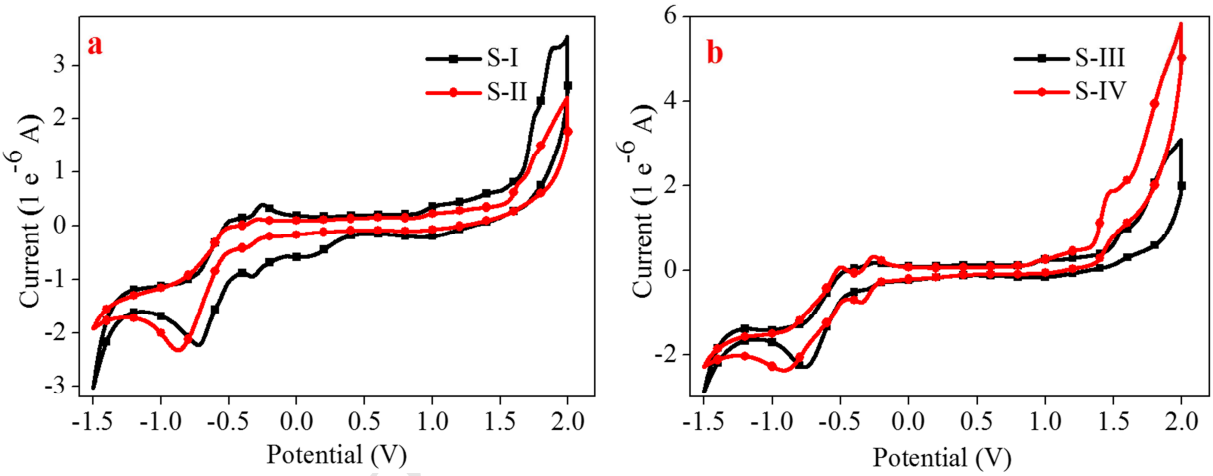
a
S-I
S-II
Current (1 e -6 A)
Potential (V)
b
S-III
S-IV
Current (1 e -6 A)
Potential (V)

Fig. 4

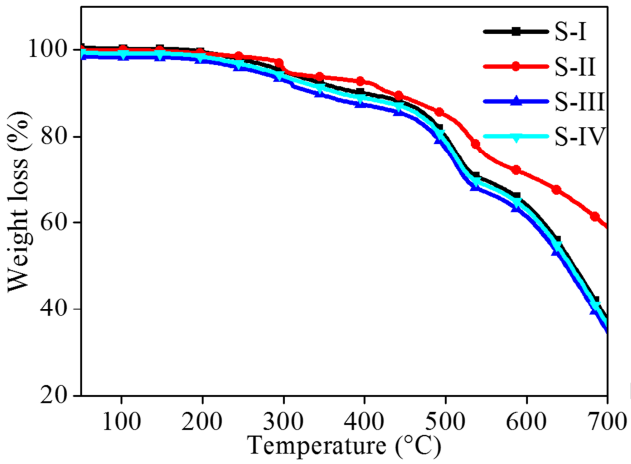
S-I
S-II
S-III
S-IV
Weight loss (%)
100
80
60
40
20
100
200
300
400
500
600
700
Temperature (°C)

Fig. 5

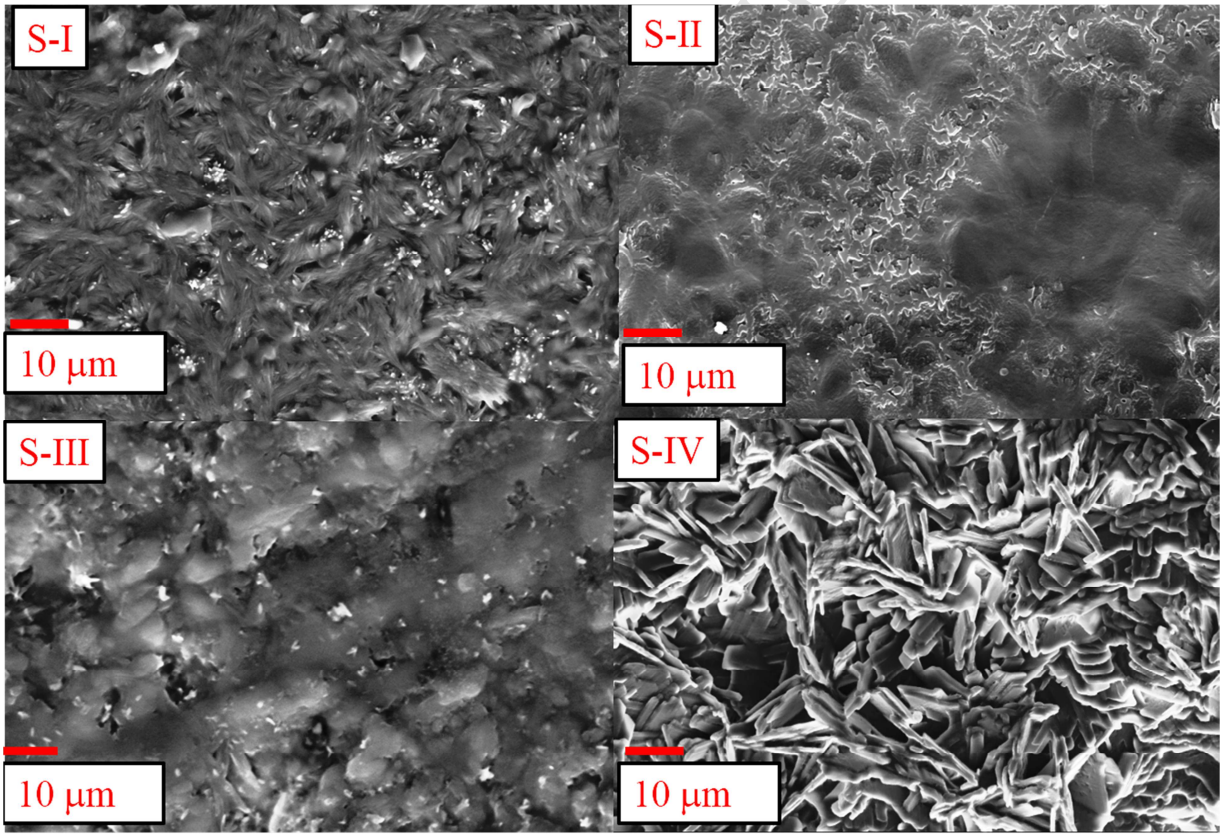
S-I
10 µm
S-II
10 µm
S-III
10 µm
S-IV
10 µm

Fig. 6

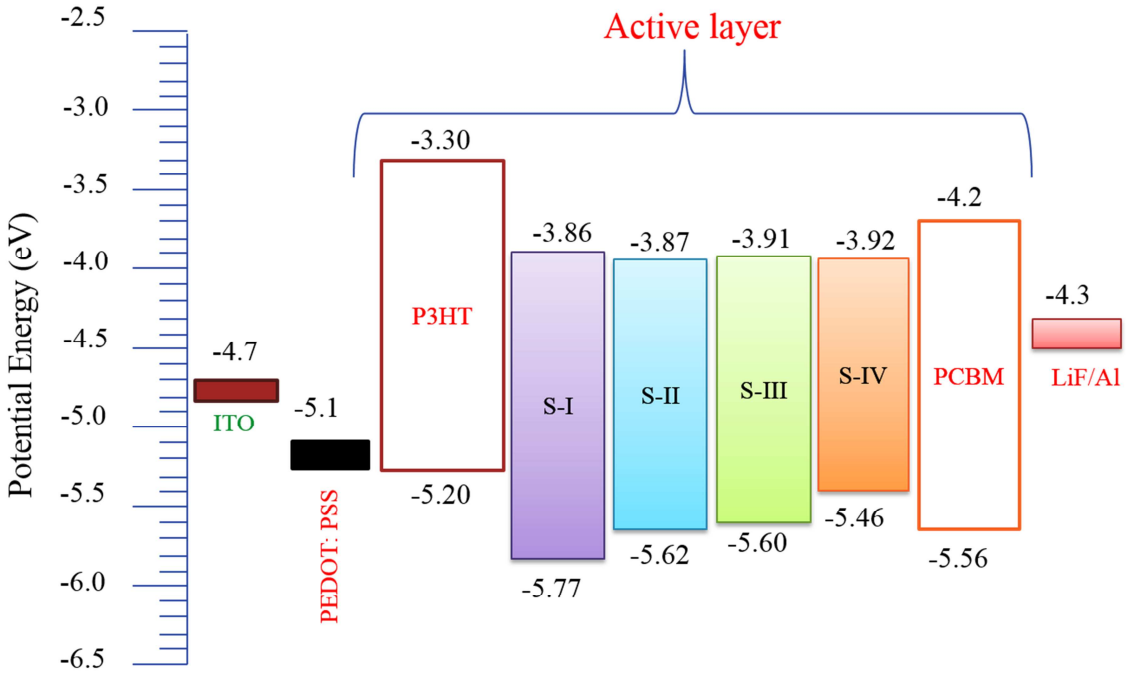
Active layer
Potential Energy (eV)
-2.5
-3.0
-3.5
-4.0
-4.5
-5.0
-5.5
-6.0
-6.5
-4.7
ITO
-5.1
PEDOT: PSS
-3.30
P3HT
-5.20
-3.86
S-I
-5.77
-3.87
S-II
-5.62
-3.91
S-III
-5.60
-3.92
S-IV
-5.46
-4.2
PCBM
-5.56
-4.3
LiF/Al

Fig. 7

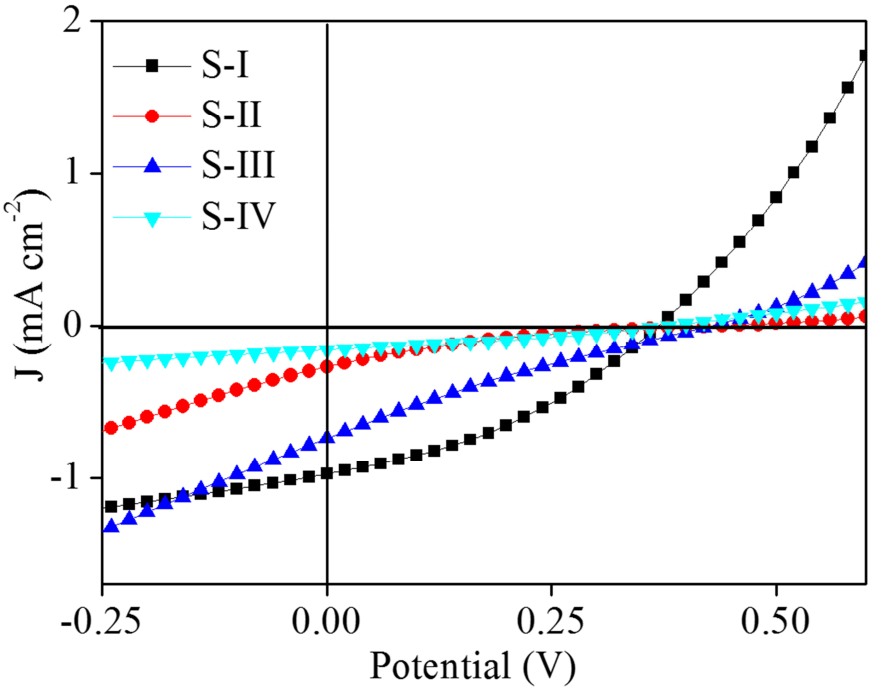
S-I
S-II
S-III
S-IV
J (mA cm-2)
2
1
0
-1
-0.25
0.00
0.25
0.50
Potential (V)

Fig. 8